Relaxation and pinning in spark-plasma sintered MgB2 superconductor

Milos Jirsa, Michal Rameš, Michael Rudolf Koblischka, Anjela Koblischka-Veneva, Kévin Berger, Bruno Douine

Relaxation and pinning in spark-plasma sintered MgB_2 superconductor.

M. Jirsa[1,#], M. Rames[1], M.R. Koblischka[2], A. Koblischka-Veneva[2], K. Berger[3], B. Douine[3]

[1]Institute of Physics ASCR, Na Slovance 2, CZ-18221 Praha 8, Czech Republic
[2]Experimental Physics, Saarland University, Campus C 63, 66123 Saarbrücken, Germany
[3]University of Lorraine, GREEN, EA 4366, BP 70239, 54506 Vandoeuvre-lès-Nancy Cedex, France

Abstract

The model of thermally activated relaxation developed and successfully tested on high-T_c superconductors [*Phys. Rev.* B **70** (2004) 0245251-9] was applied to magnetic data of a bulk spark-plasma sintered MgB_2 sample to elucidate its magnetic relaxation behavior. MgB_2 and the related borides form a superconductor class lying between classical and high-T_c superconductors. In accord with this classification, the relaxation phenomena were found to be about ten times weaker than in cuprates. Vortex pinning analyzed in terms of the field dependence of the pinning force density indicates a combined pinning by normal point-like defects and by grain surfaces. An additional mode of pinning at rather high magnetic fields (of still unknown origin) was observed.

PACS numbers: 74.25 Ha; 74.25 Sv; 74.25 Wx; 74.70 Ad; 74.81.Bd

Key words: Bulk MgB2 superconductor, magnetic properties, magnetic relaxation, critical currents, pinning force density.

[#] Corresponding author, e-mail: jirsa@fzu.cz

1. Introduction.

MgB_2 and the related borides form a superconductor class set between classical and high-T_c superconductors [1-5]. The critical temperature is moderate (39 K), but the material possesses some specific properties that make it useful and attractive for applications; it is cheap and free of rare earth elements, it is easy to prepare and exhibits quite high critical current densities up to high magnetic fields. The great advantage of MgB_2 is that in polycrystalline form grain boundaries are not obstacles for current flow. [6,7] Immediately after the discovery of superconductivity in MgB_2 [8] the new material was subjected to an intensive research. Its results were summarized e.g. in the topical review of Buzea and Yamashita [4] and can be found in a number of references therein.

High critical current density, J_c, and the upper critical magnetic field, B_{c2}, are always two principal requirements as regards applications. In high-T_c superconductors the huge magnetic relaxation reduces the irreversible magnetic moment, the associated current density and the irreversibility field[1]. [9] As the relaxation is in general logarithmic in time [10], after some time J_c relaxes to a nearly stable level determined by the effective pinning barrier and Lorentz force. The conventional way of studying this phenomenon is based on the measurement of the time dependence of the magnetic moment induced by a preceding fast change of magnetic field [10]. In this case we face the problem of unknown time scale origin. To avoid this, one has to set the initial time quite high and to measure for a long time period. Testing the relaxation properties in this manner in a wide field and temperature range is time consuming. A significantly faster alternative is the dynamic relaxation [11] associated with the sensitivity of the magnetization loop size to the field sweep rate [12]. In this case it is enough to measure two magnetization loops at each temperature with different field sweep rates. In this way one obtains relaxation characteristics in the whole field range [13]. Both conventional and dynamic relaxations have been investigated on various forms of MgB_2 by a number of researchers [14-19]. The magnetic relaxation was found much weaker than in cuprates. Rather surprising in this context is the relatively low value of irreversibility field with respect to upper critical field [14-17].

In the present paper we report the relaxation phenomena and pinning analyses of a dense bulk MgB_2 superconductor prepared by spark-plasma sintering method, together with the electron backscatter diffraction (EBSD) showing the grain disorientation distribution on a mechanically polished sample surface. Relaxation was investigated by means of dynamic relaxation method.

---

[1] In the static model the irreversibility line is defined by equilibrium between pinning force and Lorentz force [10]. This approach was used for weakly relaxing classical superconductors. In HTSC, huge relaxation makes the induced irreversible magnetic moment, the hysteresis loop size, the associated J_c, and the irreversibility line sensitive to thermal activation and their actual values are given by equilibrium between magnetic induction (depending on magnetic field sweep rate) and relaxation (i.e. thermal activation and the actual pinning potential). As a result, the irreversibility field (in general) varies with the field sweep rate [11-13].

2. Experimental details

Bulk MgB_2 sample of 20 mm diameter and 9.7 mm height was prepared using spark-plasma sintering under 50 MPa pressure [20]. The sample density reached 99.2 % of the theoretical value. The reaction temperature was 1200 °C. X-ray diffraction analysis revealed additional peaks of the MgB_4 phase, which could provide additional flux pinning sites. Prior to the present analysis, trapped field in the field-cooling mode was measured on the sample. It reached 2.98 T at 20 K [21].

The magnetic measurements were performed with a vibrating sample magnetometer (VSM), a part of the PPMS facility with 9 Tesla magnet. The sample for magnetic measurements was a platelet of dimensions 1.5 × 1.5 × 0.5 mm^3, cut from the bulk pellet. The field sweep rates dB/dt = 1.15 T/min, 0.24 T/min, and 0.12 T/min were used. The measurements were done at three temperatures, 10 K, 20 K, and 30 K. The critical current density J_c was calculated by means of the extended Bean formula [22,23]

$$J_c = 2\Delta M / \left[a\left(1 - a/3b\right)\right] , \quad (1)$$

where ΔM is difference of the signals measured on the upper and lower branch of the magnetization loop, respectively, in terms of volume magnetization, $M = m/V$, where m is the measured magnetic moment, and $V = abc$ is the sample volume. a and b are the lateral sample dimensions, $a < b$, and c is the sample thickness. The measurements were performed with magnetic field normal to the platelet's plane.

Formula (1) was derived for an isotropic homogeneous material, while our measured sample is granular with grains randomly oriented as documented by the electron backscatter diffraction (EBSD) image of the mechanically polished sample surface, Fig. 1. This inverse pole figure map in the (001)

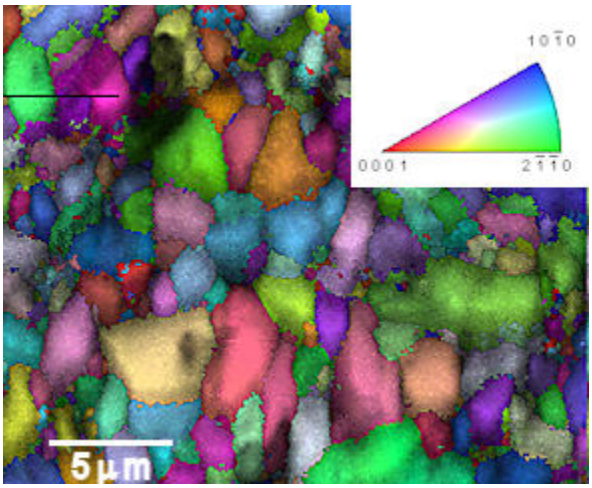

Figure 1. (Color online) EBSD inverse pole figure map in (001)-direction of the surface of the MgB2 bulk material revealing the grain size, the grain boundaries and the orientation distribution.

direction illustrates the grain sizes, the grain boundaries, and the orientation distribution. The EBSD image shows a dense structure of randomly oriented grains in the prevailing size of a few micrometers. A close inspection reveals also a number of small, submicron particles, mostly at the grain boundaries. There are nearly no pores (black or shadow spots), which indicates high density and a good quality of the material. The quality is also supported by the high critical temperature, reaching 39 K. More details on the EBSD analysis of MgB_2 bulks are given in Ref. [24].

This structural analysis leads to the conclusion that the measured magnetic moment represents a value averaged over a distribution of *c*-axis angles and grain sizes, resulting from a combined action of intra- and inter-granular currents, flowing on various loop scales. The same applies for the associated critical current density calculated from formula (1).

3. Experimental results

Figure 2 (a) presents the field dependence $J_c(B)$ measured at 10 K, 20 K, and 30 K, at each temperature with three different field sweep rates, 1.15 T/ min, 0.23 T/min, and 0.06 T/min. The magnetic hysteresis loops' height and the corresponding J_c should vary in dependence of the field sweep rate value [11-13]. However, in contrast to cuprates, the magnetic relaxation in MgB_2 appears to be so weak that the curves for the three different field sweep rates practically collapsed to one for each of the temperatures. This collapse is, however, not exact, as documented by the blow-up shown in Fig. 2 (b). Though tiny, the difference in J_c enables evaluation of the effective relaxation rate. The $J_c(B)$ maximum for 10 K, shifted from zero field upwards [Fig. 2 (a)], is an artifact caused by an incomplete flux reversal on the ascending field branch of the magnetization loop. The data at this temperature are relevant only above 0.5 T.

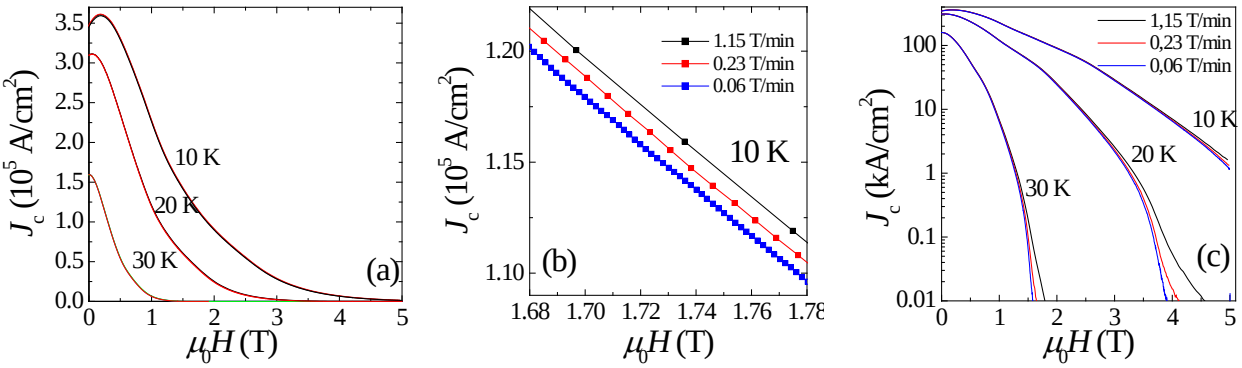

Figure 2. (Color online) (a) $J_c(B)$ dependence for the three indicated temperatures. Each of the three curves consists of three nearly overlapping curves corresponding to different field sweep rates as shown in detail in (b) for T = 10 K. (c) The semi-logarithmic representation of the data from Fig. (a) shows a variation of the irreversibility field with magnetic field sweep rate.

For the $J_c(B)$ curves lying so close to each other any spurious shift might significantly affect the data analysis. A finite time constant of the VSM set-up causes a tiny time difference in reading magnetic field

and magnetic moment data and it results in a certain shift of the $M(B)$ curve, depending on the actual field sweep rate. The correction of this effect consists of the appropriate shift of the magnetic moment time scale with respect to that of the magnetic field. In our case, the correction achieved 1.7 s, but its value is specific to each measuring set-up. The calculation was done by matrix manipulation of the original measured data set in Mathematica.

The normalized logarithmic dynamic relaxation rate is defined as

$$Q = \frac{\partial \ln J_c}{\partial \ln\left(\frac{dB}{dt}\right)} \ . \tag{2}$$

It can be rewritten as

$$Q = \frac{\frac{dB}{dt}}{J_c}\frac{\partial J_c}{\partial \frac{dB}{dt}} \ , \tag{3}$$

where the partial derivative can be replaced by ratio of small differences,

$$Q = \frac{\frac{dB}{dt}}{J_c}\frac{\Delta J_c}{\Delta \frac{dB}{dt}} . \tag{4}$$

Both dB/dt and $\Delta(dB/dt)$ are constant for the given experiment. J_c can be taken as the mean value of the two adjacent $J_c(B)$ curves recorded with different field sweep rates and ΔJ_c is difference of these two curves. In this way, two magnetization loops measured at different field sweep rates provide direct information on the relaxation behavior in the whole investigated field range. We note that the dynamic logarithmic relaxation rate is equivalent to the conventional normalized logarithmic relaxation rate, $S = -\frac{dlnJ_c}{dlnt}$, where t is the relaxation time [10,11,14-19]. It can be seen in Table 1, where our results are compared to those of conventional relaxation in Ref. [18], (Fig.2). In all cases the values are quite close to

T (K)	$B(T)$	S [18]	Q
10	1.5	0.0034	0.0042
	3	0.012	0.0138
	4	0.019	0.0296
20	1.5	0.011	0.0078
	3	0.06	0.065
	4	0.22	>1

Table 1. Comparison of the dynamic relaxation rate Q and the conventional relaxation rate S.

each other or at least in the same order.

The critical current density in Eqs. (2) - (4) can be replaced by expression (1). The geometrical factor from Eq. (1) cancels out by derivation, so as J_c in formulas (2) - (4) can be directly replaced by ΔM or

Δm. The $Q(B)$ dependences obtained in this way using the data acquired with the sweep rates 0.23 T/min and 0.06 T/min are displayed in Fig. 3.

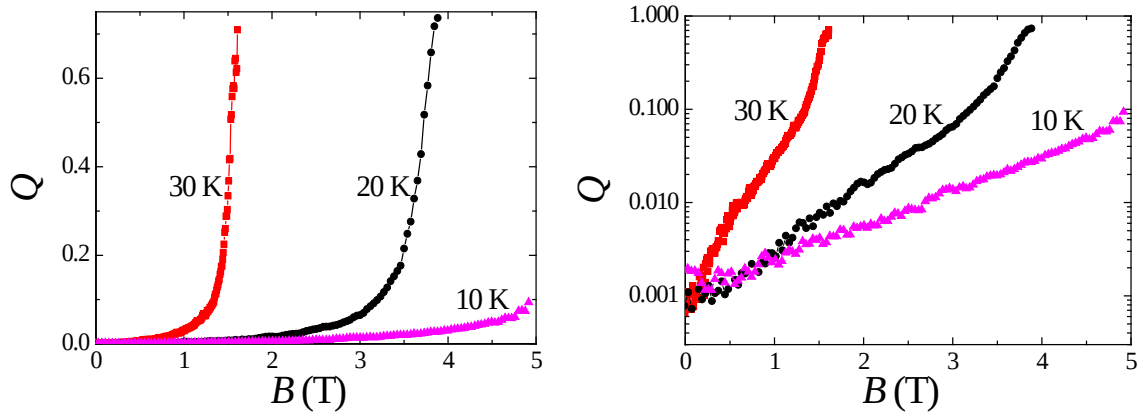

Figure 3. (Color online) Field dependences $Q(B)$ for 10 K, 20 K, and 30 K, left with linear Q scale, right in the semi-logarithmic representation.

The left panel shows $Q(B)$ dependences in the linear representation, the right panel in semi-logarithmic one. The data in Fig. 3 left indicate that the relaxation in MgB_2 is rather weak in a wide field range, only in vicinity to irreversibility field it dramatically raises. Fig. 3 right shows that Q is an exponential function of magnetic field, with two different slopes. At high magnetic fields, though exponential, the slope of the curves is still finite, indicating thus that the irreversibility field value depends on a precision criterion.

The low-field Q value, ascribed in cuprates to quantum creep [25,26], lies here around 0.001 for all three temperatures. It is by order of magnitude lower than the typical values observed in cuprates. Surprisingly, the relaxation character (shape of the $Q(B)$ dependence) does not nearly change with increasing thermal activation between 10 K and 30 K. We found that the $Q(B)$ dependence scales well

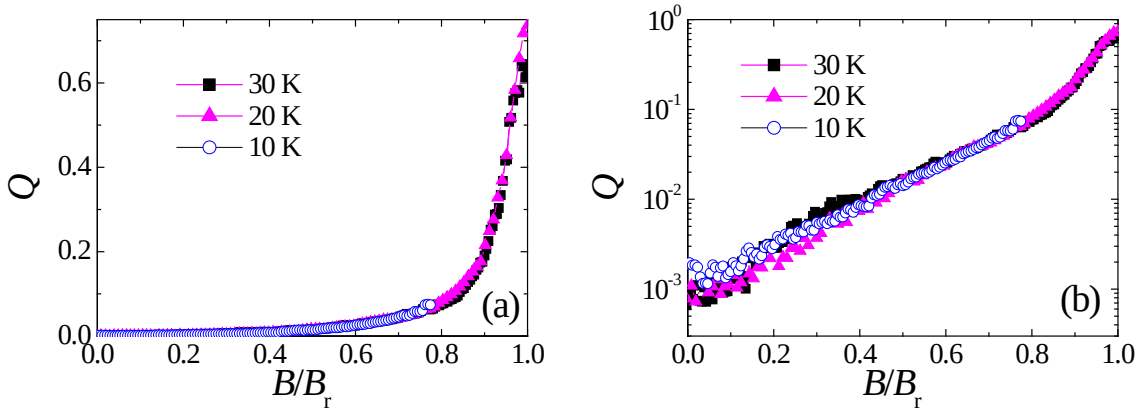

Figure 4. (Color online) The normalized logarithmic relaxation rate as a function of the normalized magnetic field B/B_r for three indicated temperatures in the linear representation (a) and the semi-logarithmic plot (b).

with the irreversibility field as documented in Fig. 4. Panel (a) shows the data in the linear representation, panel (b) in the semi-logarithmic one. The reference field, B_r, was defined by $Q(B_r)= 0.75$ (for 30 K and 20 K); for 10 K the corresponding B_r value was obtained by fitting the $F_n(b)$ curve to the other two at high

magnetic fields, 4-5 T. The resulting B_r values were 1.6 T, 3.88 T, and 6.3 T, respectively. These B_r values are slightly lower than those obtained from $J_c(B)$ dependences using the criterion J_c=10 A/cm^2 [see Fig. 2 (c)]. The B_r can be regarded as the irreversibility field.

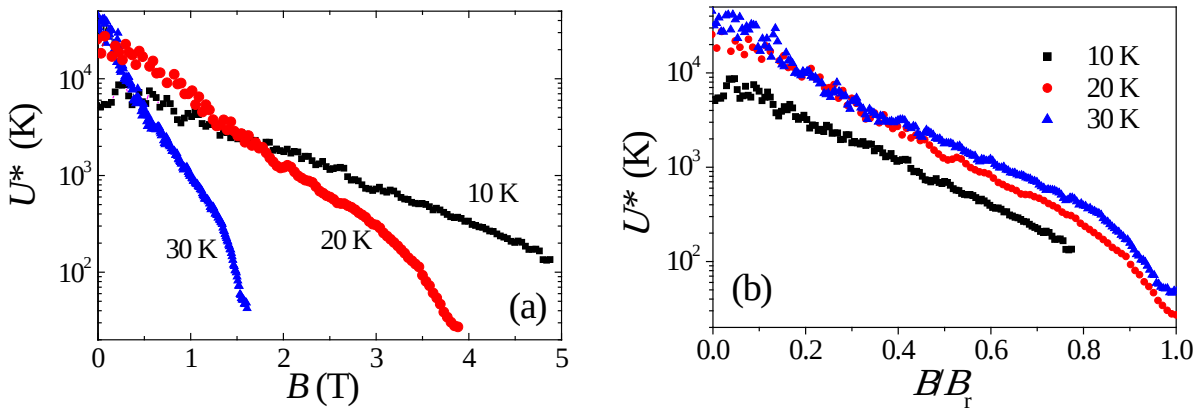

Figure 5. (Color online) The effective activation energy $U^*=T/Q$ as a function of magnetic field (a) and as a function of the normalized magnetic field (b), both in semi-logarithmic representations.

The relaxation rate Q relates to the effective activation energy, U^*, as $Q=T/U^*$.[19,27] The activation energy as a function of magnetic field is displayed in Fig. 5. For all three temperatures the activation energy is in nearly entire field range an exponential function of magnetic field and it is always significantly higher than the thermal activation, only in vicinity if the irreversibility line both energies become close to each other. This behavior supports the above conclusions on weak relaxation in our MgB_2. Relatively, in respect of the thermal activation energy, the pinning barrier is in MgB_2 much higher than in cuprates. This result is in accord with the fact that the coherence length and thus also the vortex core size are in MgB_2 about 20 times larger than in cuprates [28] and with vortex core size increases also the condensation energy gain due to pinning. The relevant pinning defect size has to be in MgB_2 much larger than in cuprates and the defects can hardly be regarded as point-like ones in the sense of “close to atomic dimensions”. Therefore, the classical approach might be appropriate for pinning analysis. We will test this idea on the normalized field dependence of the effective pinning force density [29]. Figure 6 (a) shows the reduced pinning force density, $F_n = F/F_{max}$, as a function of magnetic field normalized to the irreversibility field, $b = B/B_{irr}$, for all three investigated temperatures and the field sweep rate 0.23 T/min. The criterion for the irreversibility field determination was $F(B_{irr})/F_{max}$ =1E-3.

Inspection of Fig. 6 (a) shows that the $F_n(b)$ curves for different temperatures are close to each other, the maximum position only slightly shifts upwards with increasing temperature. A similar result was observed also on other bulk MgB_2 samples prepared by different technologies, e.g. in Ref. [30]. Note that

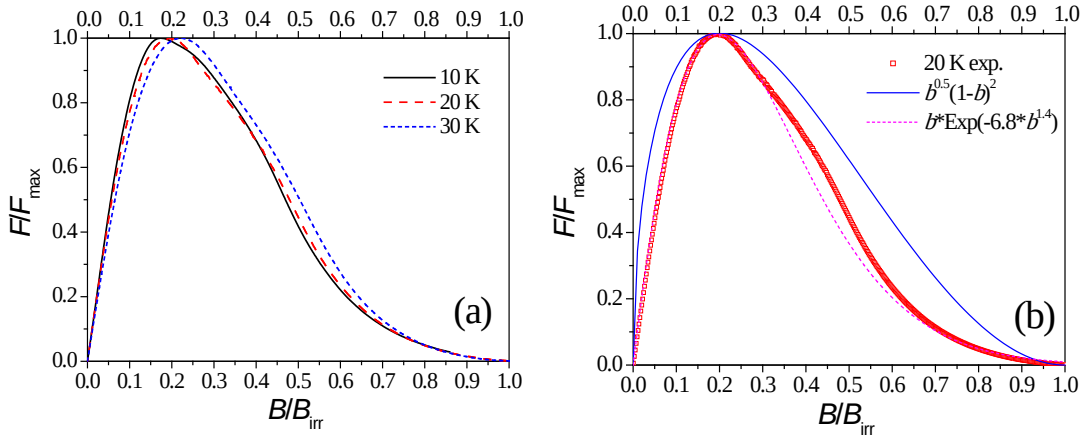

Figure 6. (Color online) (a) The reduced pinning force density as a function of magnetic field normalized to the irreversibility field, for three indicated temperatures and field sweep rate 0.23 T/min, (b) the curve for T = 20 K, together with different model functions.

the normalized curves in Fig. 6 (a) collapse both at low and high magnetic fields to a single curve. The maximum is always close to b = 0.2 but slightly shifted to higher positions with increasing temperature. According to D. Dew-Hughes [29] the maximum position b_{max} of the $F_n(B) \propto b^p(1-b)^q$ dependence, $b_{max} = \frac{p}{p+q}$, can be taken as a qualification feature for determining the prevailing pinning mechanism. According to this model, the peak position at 0.2 relates to the vortex core pinning on the surface of normal defects, described by the functional dependence with p = 0.5 and q = 2. In the present material this pinning mechanism would correspond to vortex pinning at grain boundaries. In Fig. 6 (b) the corresponding model function is displayed as a solid line. It is evident that this function in its original form is too broad. However, the classical model was developed for isotropic materials. In the granular MgB_2 anisotropy and current percolation play important roles, which can significantly slenderize the curve and shift it to a lower position [31]. Taking into account a potential effect of anisotropy and current percolation, we have to infer that the peak position for an isotropic material would lie above 0.2, corresponding to e.g. pinning by "point-like" defects (p=1, q=2, b_{max}=0.33). Note that p=1 is the limiting value to obtain $J_c(b) \propto b^{p-1}(1-b)^q$ as a continuously decreasing function of magnetic field as observed in the experiment. The results for other field sweep rates and temperatures were similar.

The difference in the peak position in Fig. 6 (a) is small. One can argue that it might be an artifact due to uncertainty in determination of the irreversibility field. To avoid this problem, Eisterer [31] suggested to normalize magnetic field with respect to the much more easily accessible field B_E defined by $F_n(B/B_E)$ = 0.5 on the high-field slope of the $F_n(b)$ curve. However, even the Eisterer's scheme did not remove the difference in $F_n(b)$ peak positions (Fig. 7). We see that the peak shifts upwards with increasing temperature. However, with increasing temperature the thermal activation of pinned vortices rises and, consequently, the smaller pins should become free of vortices and the mean vortex occupation should shift

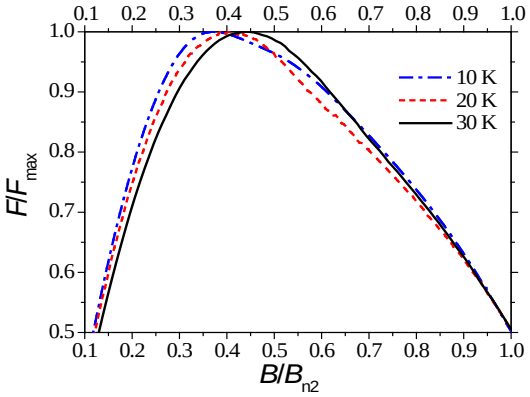

Figure 7. (Color online) The $F_n(b_n)$ dependences displayed as a function of magnetic field normalized with respect to the corresponding B_E for different temperatures.

towards larger (stronger) pinning sites; the $F_n(b)$ peak should shift to lower positions, in contradiction to the present observation. This paradox is can be explained by taking into account anisotropy of MgB_2. The anisotropy changes with temperature as $\gamma\ (T) = \gamma^* + k(1-T/Tc)$, where $\gamma^* = 1.87$ is the effective mass anisotropy and $k = 6$ [32]. Thus, at 10 K $\gamma = 6.33$, while at 30 K $\gamma = 3.25$. With decreasing anisotropy the $F_n(b)$ peak shifts to a higher position, in accord with our observations. Thus, in MgB_2 the $F_n(b)$ peak shift due to thermal activation is masked by a stronger change of the effective anisotropy (the effect of percolation was shown to be small [31]).

In general, the position of the $F_n(b)$ peak indicates pinning somewhere between normal "point-like" defects (it means those comparable in size with vortex core) and surface pinning at the grain boundaries. The possible candidates for the "point-like" defects are precipitates of the MgB_4 phase and MgO_2 detected by X-ray diffraction analysis. The shoulder on the high-field slope of the $F_n(b)$ curve reflects an additional pinning process that cannot be described by any of the mentioned models and requires a further study.

4. Summary

Magnetic relaxation in spark-plasma sintered MgB_2 was studied by means of the dynamic relaxation method developed for study of cuprates (exhibiting giant relaxation effect [9]). The normalized logarithmic relaxation rate $Q(B)$ was in the remanent state (zero magnetic field) about twenty times lower than in cuprates and increased exponentially with magnetic field up to vicinity of irreversibility field. There, the $Q(B)$ dependence became even faster. This behavior was similar for all three investigated temperatures. The $Q(B)$ dependence scaled well with the irreversibility field. The effective activation energy appeared to be for all three temperatures and for nearly entire field ranges significantly higher than the thermal energy, in accord with the weak relaxation effect observed.

We attempted to interpret the experimental normalized pinning force density as a function of magnetic field, $F_n(b)$, using the classical power-law model for an isotropic homogeneous superconductor [29]. The original approach, developed for isotropic superconductors, was not much successful: the curves were too

broad. The narrower experimental $F_n(b)$ dependence can be attributed to the anisotropy of the material in the polycrystalline MgB_2 sample [31]. Taking the effect of anisotropy into account, the observed $F_n(b)$ peak position close to b=0.2 should effectively correspond to some pinning process with a higher position of the peak in an isotropic homogeneous sample. Such a mechanism might be "core pinning on normal "point-like" defects" [29] (b=0.33). These defects might be precipitates of MgB_4 and MgO_2 detected by X-ray diffraction analysis but not seen directly on the EBSD inverse pole figure map, if their average size would be close to the vortex core dimension. Peak of the $F_n(b)$ dependence shifted up-wards with increasing temperature, which contradicted to the expected increase of thermal activation and the associated shift of the vortex occupation to larger defects. A similar behavior was also observed on other MgB_2 samples prepared by different technique [30,33]. We attributed this effect to the temperature dependence of anisotropy. A shoulder observed on the high-field slope of the $F_n(b)$ dependence represents an additional high-field pinning process. This process requires a further investigation.

Acknowledgements

We thank J. Noudem (CRISMAT, Caen, France) for providing the MgB_2 sample employed in this study. The collaboration Saarbrücken-Nancy is supported by an EU-INTERREG project Greater Region Magnetism Network (GRMN), which is gratefully acknowledged.

References

[1] Vinod K, Abhilash Kumar R G, Syamaprasad U 2007 *Supercond. Sci. Technol.* **20** R1

[2] Tomsic M, Rindfleisch M *et al*. 2007 *Int. J. Appl. Ceram. Technol.* **4** 250

[3] Mikheeko P, Martinez E, Bevan A, Abell J S, MacManus-Driscoll J 2007 *Supercond. Sci. Technol.* **20** S264

[4] Buzea C, Yamashita T 2001 *Supercond. Sci. Technol*. **14** R115

[5] Scanlan R M, Malozemoff A P, Larbalestier D C 2004 *Proc. IEEE* **92** 1639

[6] Larbalestier D C *et al*. 2001 *Nature* **410** 186

[7] Kawano K, Abel J S, Kambara M, Hari Babu N, Cardwell D A, 2001 *Apl. Phys. Lett.* **71** 2216

[8] Nagamatsu J, Nakagawa N, Muranaka T, Zenitani Y, Akimitsu J 2001 Nature (London) **410** 63

[9] Yeshurun Y, Malozemoff A P 1988 *Phys. Rev. Lett.* **60** 2202

[10] Anderson P W, Kim Y B 1964 *Rev. Mod. Phys.* **36** 39

[11] Jirsa M, Půst L, Schnack H G, Griessen R 1993 *Physica* C **207** 85

[12] Půst L, Kadlecová J, Jirsa M, Durčok S 1990 *J. Low Temp. Phys.* **78** 179

[13] Jirsa M, Nishizaki T, Kobayashi N, Muralidhar M, Murakami M 2004 *Phys. Rev.* B **70** 0245251

[14] Wen H H, Li S L, Zhao Z W, Jin H, Ni Y M, Kang W N, Kim Hyeong-Jin, Choi Eum-Mi, Lee Sung-Ik 2001 *Phys. Rev.* B **64** 134505

[15] Wen H H, Li S L, Zhao Z W, Jin H, Ni Y M, Ren Z A, Che G C, Zhao Z X 2001 *Physica* C **363** 170-178

[16] Wen H H, Li S L, Zhao Z W, Jin H, Ni Y M, Ren Z A, Che G C, Zhao Z X 2002 *Supercond. Sci. Technol.* **15** 315–319

[17] Zhao Z W, Wen H H, Li S L, Ni Y M, Ren Z A, Che G C, Yang H P, Liu Z Y, Zhao Z X 2001 *Chinese Physics* **10** 340

[18] Martinez E, Navaro R 2004 *Apl. Phys. Lett.* **85** 1382

[19] Miu L, Ivan I, Aldica G, Badica P, Groza J R, Miu D, Jakob G, Adrian H 2008 *Physica* C **486** 2279

[20] Noudem J G, Aburras M, Bernstein P, Chaud X, Muralidhar M, Murakami M 2014 *J. Appl. Phys.* **116** 163916

[21] Berger K, Koblischka M R, Douine B, Noudem J, Bernstein P, Hauet T, Lévêque J 2015 presented at EUCAS 2015, 6.9.-10.9.2015, Lyon, France, submitted to *IEEE Trans.Appl. Supercond.*

[22] Koblischka-Veneva A, Koblischka M R, Schmauch J, Inoue K, Muralidhar M, Berger K, Noudem J 2015 presented at PASREG 2015, 2.9.-4.9.2015, Liège, Belgium, submitted to *Supercond. Sci. Technol.*

[23] Bean C P 1964 *Rev. Mod. Phys*. **36** 2489

[24] Chen D X and Goldfarb R B 1989 *J. Appl. Phys*. **66** 2489

[25] Hoekstra A, Martinez J C**,** Griessen R 1994 *Physica* C **235-240** 2955

[26] Åkerman J J *et al*. 2001 *Phys. Rev*. B **64** 094509

[27] Yeshurun Y, Malozemoff A P, Shaulov A 1996 *Rev. Mod. Phys*. **68** 911

[28] Loudon J C *et al.* 2015 *Phys. Rev*. B **91** 054505

[29] Dew-Hughes D 1974 *Philos. Mag.* **30** 236-305

[30] Koblischka M R *et al*. 2014 *IEEE Trans. Magn*. **50** 9000504

[31] Eisterer M 2008 *Phys. Rev.* B **77** 144524

[32] Shi Z X *et al.* 2003 *Phys. Rev.* B **68** 104513

[33] Wiederhold A *et al*. 2015 presented at EUCAS 2015, 6.9.-10.9.2015, Lyon, France, submitted to *IEEE Trans. Appl. Supercond*. and WA bachelor thesis, Saarland University, Saarbrücken, 2015, unpublished